# Efficient and Low-Backaction Quantum Measurement Using a Chip-Scale Detector

Eric I. Rosenthal, Christian M. F. Schneider, Maxime Malnou, Ziyi Zhao, Felix Leditzky, Benjamin J. Chapman, Waltraut Wustmann, Xizheng Ma, Daniel A. Palken, Maximilian F. Zanner, Leila R. Vale, Gene C. Hilton, Jiansong Gao, Graeme Smith, Gerhard Kirchmair, and K. W. Lehnert

Phys. Rev. Lett. **126**, 090503 — Published 3 March 2021
DOI: 10.1103/PhysRevLett.126.090503

# Efficient and low-backaction quantum measurement using a chip-scale detector

Eric I. Rosenthal,[1,2,3,*] Christian M. F. Schneider,[4,5] Maxime Malnou,[2,3] Ziyi Zhao,[1,2,3]
Felix Leditzky,[1,3,6] Benjamin J. Chapman,[7] Waltraut Wustmann,[8] Xizheng Ma,[1,2,3]
Daniel A. Palken,[1,2,3] Maximilian F. Zanner,[4,5] Leila R. Vale,[3] Gene C. Hilton,[3]
Jiansong Gao,[2,3] Graeme Smith,[1,2,3,6] Gerhard Kirchmair,[4,5] and K. W. Lehnert[1,2,3]

[1] *JILA, University of Colorado, Boulder, Colorado 80309, USA*
[2] *Department of Physics, University of Colorado, Boulder, Colorado 80309, USA*
[3] *National Institute of Standards and Technology, Boulder, Colorado 80305, USA*
[4] *Institute for Quantum Optics and Quantum Information of the Austrian Academy of Sciences, A-6020 Innsbruck, Austria*
[5] *Institute for Experimental Physics, University of Innsbruck, A-6020 Innsbruck, Austria*
[6] *Center for Theory of Quantum Matter, University of Colorado, Boulder, Colorado 80309, USA*
[7] *Department of Applied Physics, Yale University, New Haven, Connecticut, 06511, USA.*
[8] *The Laboratory for Physical Sciences, College Park, Maryland 20740, USA*

(Dated: January 25, 2021)

Superconducting qubits are a leading platform for scalable quantum computing and quantum error correction. One feature of this platform is the ability to perform projective measurements orders of magnitude more quickly than qubit decoherence times. Such measurements are enabled by the use of quantum-limited parametric amplifiers in conjunction with ferrite circulators — magnetic devices which provide isolation from noise and decoherence due to amplifier backaction. Because these non-reciprocal elements have limited performance and are not easily integrated on-chip, it has been a longstanding goal to replace them with a scalable alternative. Here, we demonstrate a solution to this problem by using a superconducting switch to control the coupling between a qubit and amplifier. Doing so, we measure a transmon qubit using a single, chip-scale device to provide both parametric amplification and isolation from the bulk of amplifier backaction. This measurement is also fast, high fidelity, and has 70% efficiency, comparable to the best that has been reported in any superconducting qubit measurement. As such, this work constitutes a high-quality platform for the scalable measurement of superconducting qubits.

Qubit-specific projective measurement is a requirement for scalable quantum computation and quantum error correction [1]. In superconducting systems, qubit measurement generally involves scattering a microwave pulse off of a readout cavity dispersively coupled to the qubit [2, 3]. This pulse is routed through ferrite circulators and/or isolators to a Josephson junction-based parametric amplifier [4–8], sent to room temperature, and digitized. This readout scheme can work well [9]: it is low-backaction, quantum non-demolition, and can have infidelity of $10^{-2}$ in less than 100 ns [10], with the best reported infidelity of less than $10^{-4}$ [11].

Challenges arise, however, as the scale and requirements of superconducting quantum systems increase. In particular, ferrite circulators are bulky and their requisite number scales linearly with the number of measurement channels. Fitting enough circulators at the base temperature stage of a cryostat is one eventual bottleneck associated with building a scalable quantum computer. Furthermore, circulators are both lossy and provide finite isolation from amplifier noise. Isolation can be improved using multiple isolators in series, but at the cost of increased resistive loss and impedance mismatches, which necessitate a stronger readout pulse in order to make a projective qubit measurement. This can be just as detrimental as amplifier backaction; both have the potential to drive higher-level state transitions which can cause readout errors, and reduce the extent to which a measurement is quantum non-demolition [12, 13].

In recognition of these problems, it has been a longstanding goal to replace ferrite circulators and isolators with a chip-scale, higher-performance alternative. Efforts to do so have often involved parametrically coupling high-Q resonant modes [14–21] or concatenating frequency conversion and delay operations [22–25]. Such technologies show promise but have yet to supplant ferrites. Performance specifications such as isolation and bandwidth must still be improved, and multiple high frequency control tones per device are undesirable from the perspective of scalability. An alternate approach is to simply remove any non-reciprocal components between the qubit and first, Josephson-junction based amplifier [26–28]. This allows for high efficiency but at the cost of significant exposure to amplifier backaction.

Here, we instead engineer a replacement for ferrites based on the coordinated operation of superconducting switches. These switches, realized by an improvement upon the design in Refs. [29, 30], are integrated into a single, chip-scale device we call a ‘Superconducting Isolating Modular Bifurcation Amplifier’ (SIMBA), Fig. 1. The SIMBA consists of a two-port parametric cavity (a Josephson parametric amplifier, JPA, based on the devices in Refs. [4, 5, 31]) with fast, low-loss and high on-off ratio superconducting switches placed on both ports. Importantly, these switches are dc-actuated, requiring no microwave control tones. Pulsed, unidirectional gain

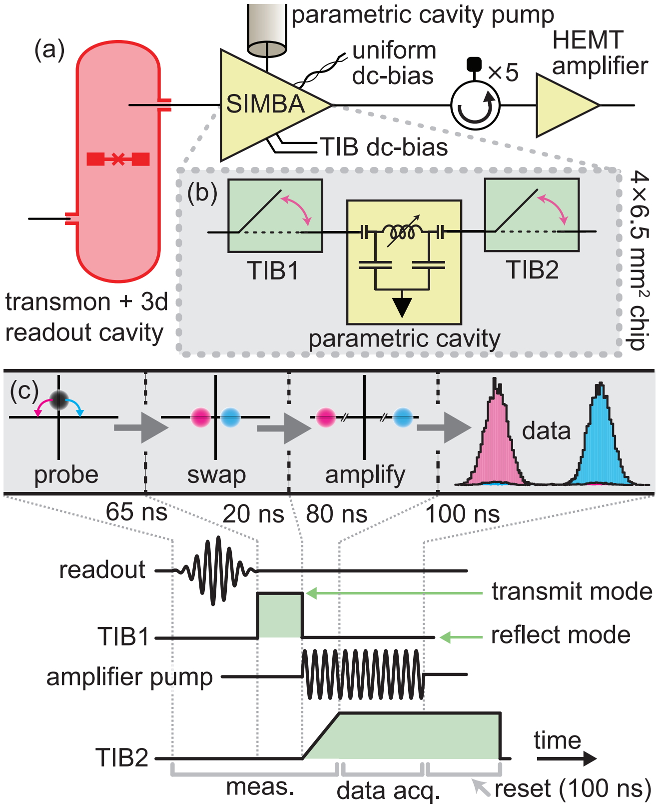


FIG. 1. **Procedure**. (a) A transmon qubit is measured using a 'Superconducting Isolating Modular Bifurcation Amplifier' (SIMBA). (b) The SIMBA is comprised of a two-port parametric cavity with a Tunable-Inductor-Bridge (TIB) style coupler on each port. (c) To measure the qubit, a probe tone is sent into the readout cavity, swapped into the parametric cavity, and then amplified. The amplified state is then coupled to a standard cryogenic measurement chain and digitized. Cyan (pink) histograms correspond to single-shot measurements when the qubit has been prepared in the ground (excited) state.

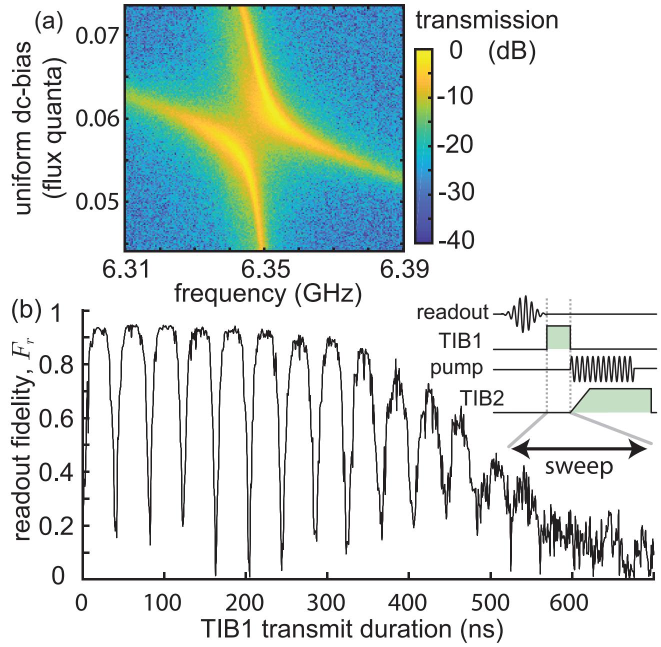


FIG. 2. **Calibration**. (a) A uniform external flux is swept while probing the readout cavity in transmission with both TIBs in transmit mode. The avoided crossing shows the parametric cavity tuning through the readout cavity. To operate a SIMBA, this uniform flux bias is set so that the readout and parametric cavities are minimally detuned. (b) Readout fidelity $F_r$ (the ability of a measurement to distinguish the qubit eigenstate, [32]), is plotted vs. the duration for which TIB1 is set to transmit mode within the measurement sequence. Oscillations with a period of 40 ns indicate coherent swapping of a readout pulse between the readout and parametric cavities.

is realized by the sequential operation of these switches combined with resonant delay, and parametric gain, in the parametric cavity. We use this procedure to demonstrate efficient, high-quality readout of a superconducting qubit while simultaneously isolating it from the bulk of amplifier backaction. We emphasize that this *procedure* is the novel idea in this work, which in the future may be implemented using a wide class of devices.

Central to the SIMBA is a flux-pumped parametric cavity: a lumped-element inductor-capacitor circuit where approximately half the inductance comes from an array of superconducting quantum interference devices (SQUIDs). The parametric cavity resonant frequency can be tuned between 4 GHz and 7.1 GHz by applying an external magnetic flux (see supplementary material Section III.D). When flux through these SQUIDs is modulated at twice the cavity resonance frequency, the cavity state undergoes phase-sensitive parametric amplification via three-wave mixing.

The external coupling of the parametric cavity is controlled by superconducting switches constructed using a 'Tunable Inductor Bridge' (TIB) [29, 33]. TIB transmission is tuned by a dc signal which changes the balance of a Wheatstone bridge of SQUID arrays. In this experiment, the speed at which transmission can be tuned is limited by off-chip, low-pass filters with a 350 MHz cutoff frequency placed on the TIB bias lines. Tested in isolation, the TIB has an on/off ratio greater than 50 dB tunable between 4 GHz and 7.3 GHz (see supplementary material Section III, which includes Refs. [34–37]). This overlaps with the range over which the parametric cavity can be tuned, allowing the SIMBA itself to be tuned to operate over several GHz. The TIB 1-dB compression point is approximately -98 dBm, which crucially allows the TIB to function effectively while the state in the parametric cavity is amplified.

We use the SIMBA to measure a transmon qubit dispersively coupled to a readout cavity. As in conventional dispersive readout [2, 3], a pulse is first sent into the weakly coupled port of a two-port readout cavity, where it acquires a qubit state-dependent phase shift. TIB1 is then set to transmit mode for a duration (20 ns), chosen to fully swap this pulse into the parametric cavity, which has previously been tuned near resonance, Fig. 2. We then strongly flux-pump the parametric cavity into the bistable regime [38–40]: a non-unitary process in which the cavity latches into one of two bistable states with opposite phase but large, equal amplitudes (see supplementary material Section IV, which includes Refs. [41–43]). Readout is achieved by seeding the parametric cavity state with the probe tone, such that the post-measurement qubit state is correlated with the latched state of the parametric cavity [44, 45]. We choose to thus discretize and store the measurement result within the cryostat as a step toward implementing rapid and hardware efficient feed-forward protocols [46]. To learn the measurement result outside of the cryostat, TIB2 is set to transmit mode, coupling this state to a standard cryogenic microwave measurement chain.

We focus on three figures of merit to describe the success of this readout: excess backaction $n_b$, measurement efficiency $\eta$, and maximum readout fidelity $F_0$. To characterize these quantities we use the framework of measurement-induced dephasing [47] (see supplementary material Section II, which includes Refs. [48–54]).

Ideally, measurement-induced dephasing of the qubit comes *only* from a readout pulse. Consider a qubit prepared in a superposition state $(|0\rangle + |1\rangle)/\sqrt{2}$; a readout pulse at the appropriate frequency interacts with this qubit to create the entangled state $(|0\rangle|\alpha_0\rangle + |1\rangle|\alpha_1\rangle)/\sqrt{2}$. Here $|\alpha_0\rangle$ and $|\alpha_1\rangle$ are coherent states both of amplitude $|\alpha|$, separated in phase space by the angle $2\theta = 2\arctan(2\chi/\kappa_r)$, where the readout cavity frequency shifts by $\pm\chi/2\pi$ dependent on the qubit state, and $\kappa_r/2\pi$ is the loss rate of the readout cavity [2, 3]. After measurement, the off-diagonal element of the qubit density matrix becomes $|\rho'_{01}| = \frac{1}{2}|\langle\alpha_0|\alpha_1\rangle| = \frac{1}{2}e^{-2n_r}$, where $n_r = (|\alpha|\sin\theta)^2$ is the effective photon number of the readout pulse, corresponding to the square of half the separation in phase space between $|\alpha_0\rangle$ and $|\alpha_1\rangle$ (see supplementary material Section II.A). Here, $n_r$ is nearly equal to the readout pulse photon number $|\alpha|^2$ because $2\chi/2\pi = 1.93\,\mathrm{MHz}$ and $\kappa_r/2\pi = 440\,\mathrm{kHz}$, so that $n_r = 0.95|\alpha|^2$.

In practice, measurement may include 'excess backaction' or *additional* dephasing. This is modeled as an additional pulse with an effective photon number,

$$n_b = -\frac{1}{2}\log(2\rho_b), \tag{1}$$

such that the coherence of a superposition state is reduced to $|\hat{\rho}'_{01}| = \frac{1}{2}e^{-2(n_b+n_r)} = \rho_b e^{-2n_r}$, where $0 \le \rho_b \le 1/2$ is the post-measurement coherence in the absence of readout photons. The effective photon number $n_r$ in a given readout pulse is not a priori known, but is related to its amplitude expressed in experimental units, $\epsilon \propto \sqrt{n_r}$. The measurement-induced dephasing can therefore be expressed as,

$$|\hat{\rho}'_{01}| = \rho_b e^{-2(\sqrt{n_r})^2} = \rho_b e^{-\epsilon^2/2\sigma^2}, \tag{2}$$

where $\sqrt{n_r} = \epsilon/2\sigma$ and physically, the constant $\sigma$ calibrates the readout pulse amplitude in units of $(\text{photon number})^{1/2}$.

A dephased qubit indicates that information about its energy eigenstate may be learned by a detector. This information may be quantified by a readout fidelity [32]

$$F_r = 1 - P(e|0) - P(g|\pi), \tag{3}$$

where $P(e|0)$ and $P(g|\pi)$ are the probability of incorrect assignment when the qubit is prepared in the ground or excited state, respectively.

For dispersive readout using a thresholded measurement (see supplementary material Section II.B), readout fidelity is

$$F_r = F_0 \mathrm{erf}\left[\sqrt{2\eta n_r}\right] = F_0 \mathrm{erf}\left[\nu\epsilon\right]. \tag{4}$$

Here $F_0$ is the maximum readout fidelity, and $\eta = \eta_{\mathrm{loss}}\eta_{\mathrm{amp}}$ is the measurement efficiency [47], defined here such that $1 - \eta_{\mathrm{loss}}$ is the fraction of readout pulse energy which has been lost before the pulse undergoes parametric amplification, which is assumed to be noiseless such that $\eta_{\mathrm{amp}} = 1$. The constant $\nu = \sqrt{2\eta n_r}/\epsilon$ characterizes how quickly $F_r$ increases with $\epsilon$.

The relationship between $\nu$ and $\sigma$ gives the convenient formula,

$$\eta = 2\sigma^2\nu^2. \tag{5}$$

Intuitively, measurement efficiency $\eta$ is determined by the readout fidelity of a weak measurement (quantified by $\nu$), compared to its backaction (quantified by $\sigma$) [55].

To experimentally determine the figures of merit $n_b$, $\eta$ and $F_0$, we measure readout fidelity and post-measurement coherence, both as functions of the experimental readout amplitude $\epsilon$. Readout fidelity $F_r$ is simply computed by measuring $P(e|0)$ and $P(g|\pi)$, and using Eq. 3. To measure $|\hat{\rho}'_{01}|$, the qubit is prepared in a superposition state, exposed to backaction from a variable strength measurement with readout pulse amplitude $\epsilon \propto \sqrt{n_r}$, and then projectively measured after a variable Ramsey delay and a second $\pi/2$ pulse, Fig. 3a. We first characterize the backaction from a 'measurement' of zero readout amplitude, $\epsilon = 0$; meaning backaction solely due to actuating the TIBs (left-most point in the 'pump off' data, cyan, Fig. 3c), and the combination of actuating the TIBs and pumping the parametric cavity (left-most data point, 'pump on' data, indigo). We then repeat this sweep over the variable amplitude $\epsilon$, both with the parametric pump turned off (cyan) and on (indigo) during

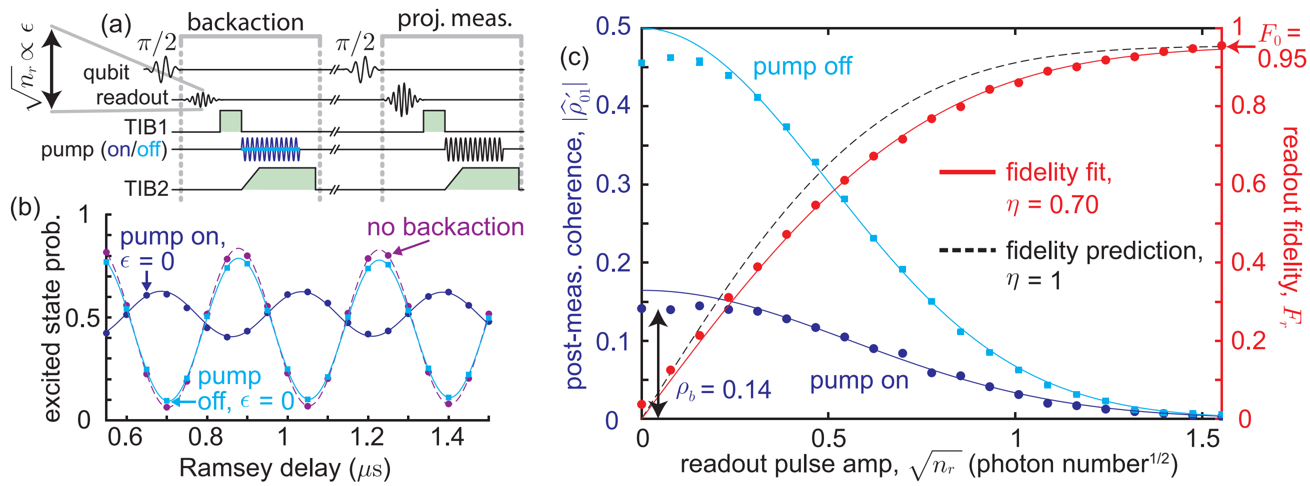


FIG. 3. **Characterization**. (a) Post-measurement qubit coherence $|\hat{\rho}'_{01}|$ is obtained by inserting a variable measurement into a Ramsey sequence, exposing the qubit to backaction. The ratio of the amplitude of the measured Ramsey fringes to the amplitude of those measured without this backaction (nothing inserted into the Ramsey sequence) equals $2|\hat{\rho}'_{01}|$. (b) Excess backaction is determined by inserting a 'measurement' with zero readout amplitude. Post-measurement coherence after excess backaction with the parametric cavity pump on (indigo) and off (cyan), are compared to a case with no backaction (no readout pulse, pump, or TIB switching inserted in the Ramsey sequence, violet). (c) Post-measurement coherence $|\hat{\rho}'_{01}|$ (left y-axis) and readout fidelity $F_r$ (right y-axis, red data points), are measured while sweeping the readout amplitude $\sqrt{n_r}$ of a variable strength measurement. As in (b), $|\hat{\rho}'_{01}|$ is measured both with the parametric pump turned on or off during the variable measurement sequence (indigo or cyan data points, respectively). Post-measurement coherence with the parametric pump turned on, but in the absence of readout photons, is specified by $\rho_b = |\hat{\rho}'_{01}(\sqrt{n_r} = 0)|$ and determines the excess backaction $n_b = -\log(2\rho_b)/2$. Measurement efficiency $\eta$ is determined by a comparison between measurement-induced dephasing and readout fidelity while sweeping readout amplitude.

the variable measurement. For comparison, qubit coherence is also measured *without* exposure to any backaction, meaning no variable measurement inserted into the Ramsey delay (e.g. violet data, Fig. 3b). The ratio of the Ramsey fringe amplitudes with/without exposure to backaction gives $2|\hat{\rho}'_{01}|$, with the ratio taken to correct for readout infidelity.

This characterization determines that our readout is low-backaction, high fidelity, and high efficiency. Excess backaction is found from $\rho_b = 0.141 \pm 0.002$ (leftmost data point, 'pump on' data, Fig. 3c. Uncertainty represents plus/minus one standard deviation). Using Eq. 1, this corresponds to $n_b = 0.63 \pm 0.01$ effective photons of excess backaction; about one quarter of the $n_r^{\text{proj}} = 2.4$ effective photons used in a projective measurement (the maximum value on the $x$-axis of Fig. 3c), and far less than the $\sim 150$ photons in the pumped state of the parametric cavity (see supplementary material Section IV.E). Next, we find $\nu$ and the maximum fidelity $F_0 = 95.5\% \pm 0.3\%$ by fitting $F_r$ vs. readout amplitude (red data, Fig. 3c) to Eq. 4. Finally we obtain $\sigma$ from a fit of the 'pump off' data (cyan) to Eq. 2, and therefore determine $\eta = 70.4\% \pm 0.9\%$ using Eq. 5. This fit excludes the first four data points, which level off more quickly than predicted such that excess backaction includes $0.05 \pm 0.01$ effective photons caused solely by actuating the TIBs [56]. This dephasing process is not captured by our model, and may result from a noise source on the parametric cavity side of TIB1 (see supplementary material Section V.B).

The limitations on $n_b$, $\eta$ and $F_0$ are understood and their values may be improved upon (see supplementary material Section VI, which includes Refs. [57–68]). Excess backaction primarily results from the $-26\,\text{dB}$ of transmission through TIB1 when in reflect mode. This transmission is higher than the $-50\,\text{dB}$ of transmission measured in a single TIB in isolation, a discrepancy which may result from the solvable problems of a spurious transmission path within the chip or sample box, or the pumped parametric cavity state approaching the power handling capability of the TIB. Maximum readout fidelity is limited by qubit decay and state preparation error including a $\sim 2\%$ thermal population, errors which do not represent limitations of the SIMBA itself. Finally, efficiency is limited primarily by the $4.0\,\text{MHz} \pm 0.2\,\text{MHz}$ loss rate of the parametric cavity. The dominant contributions to this loss are the non-zero transmission through TIB2 when in reflect mode, on-chip dissipation, and coupling to cable modes: effects which may all be mitigated in future designs.

In conclusion, we measure a transmon qubit using a chip-scale, pulsed directional amplifier. The qubit is isolated from amplifier backaction using a superconducting switch to control the coupling between a readout and

TABLE I. **Readout performance summary.**

| Parameter | Value |
|---|---|
| Measurement efficiency | $\eta = 70.4\% \pm 0.9\%$ |
| Excess backaction | $n_b = 0.66 \pm 0.01$ photons |
| Maximum readout fidelity | $F_0 = 95.5\% \pm 0.3\%$ |
| Measurement time | 265 ns |

parametric cavity. Simultaneously demonstrated metrics for this readout are given in Table I. With reasonable changes to the SIMBA and experimental setup, we estimate it is possible to achieve $\eta > 90\%$ with $F_0 > 99\%$, $n_b \leq 0.02$ and a measurement time of less than 100 ns (see supplementary material Section VI).

This demonstration combines state-of-the-art measurement efficiency *and* considerable isolation from amplifier backaction such that $n_b \sim n_r^{\text{proj}}/4$. The measurement efficiency of previous superconducting qubit readout schemes have been limited to $\eta = 80\%$ [27], and less when providing any isolation before a parametric amplifier [10, 21, 31, 69] (see supplementary material Section I, which includes Refs. [70–76], for a broader comparison to other works). Near-unit measurement efficiency after future improvements would allow for near-*complete* access to the information extracted from a quantum system. Additionally, the SIMBA is chip-scale, compatible with scalable fabrication procedures including the use of through-silicon-vias [77], and requires only one microwave control tone to operate. The SIMBA is therefore a favorable choice for high-quality and scalable superconducting qubit measurement.

*Acknowledgments* — The authors thank Florent Lecocq, Alexandre Blais, Jonathan Gross and K. D. Osborn for helpful discussions, and thank James Uhrich, Calvin Schwadron and Kim Hagen for help in the design and fabrication of the mechanical parts used in this experiment. This work is partially supported by the Air Force Office of Scientific Research Multidisciplinary Research Program of the University Research Initiative (AFOSR MURI) under grant number FA9550-15-1-0015, the Army Research Office (ARO) under contract W911NF-14-1-0079 and the National Science Foundation under Grant Number 1734006. E.I.R acknowledges support from the ARO QuaCGR fellowship and C.S. and M.Z. acknowledge support from the Austrian Science Fund FWF within the DK-ALM (W1259-N27).

* eric.rosenthal@colorado.edu

[1] David P. DiVincenzo, "The physical implementation of quantum computation," Fortschr. Phys. **48**, 771–783 (2000).

[2] Alexandre Blais, Ren-Shou Huang, Andreas Wallraff, S. M. Girvin, and R. J. Schoelkopf, "Cavity quantum electrodynamics for superconducting electrical circuits: An architecture for quantum computation," Physical Review A **69**, 062320 (2004).

[3] Alexandre Blais, Arne L. Grimsmo, and Andreas Wallraff, "Circuit quantum electrodynamics," arXiv:2005.12667 (2020).

[4] M. A. Castellanos-Beltran and K. W. Lehnert, "Widely tunable parametric amplifier based on a superconducting quantum interference device array resonator," Applied Physics Letters **91**, 083509 (2007).

[5] T. Yamamoto, K. Inomata, M. Watanabe, K. Matsuba, T. Miyazaki, W. D. Oliver, Y. Nakamura, and J. S. Tsai, "Flux-driven josephson parametric amplifier," Applied Physics Letters **93**, 042510 (2008).

[6] N. Bergeal, R. Vijay, V. E. Manucharyan, I. Siddiqi, R. J. Schoelkopf, S. M. Girvin, and M. H. Devoret, "Analog information processing at the quantum limit with a Josephson ring modulator," Nature Physics **6**, 296–302 (2010).

[7] C. Macklin, K. O'Brien, D. Hover, M. E. Schwartz, V. Bolkhovsky, X. Zhang, W. D. Oliver, and I. Siddiqi, "A near–quantum-limited Josephson traveling-wave parametric amplifier," Science **350**, 307–310 (2015).

[8] N. E. Frattini, U. Vool, S. Shankar, A. Narla, K. M. Sliwa, and M. H. Devoret, "3-wave mixing josephson dipole element," Applied Physics Letters **110**, 222603 (2017).

[9] Evan Jeffrey, Daniel Sank, J. Y. Mutus, T. C. White, J. Kelly, R. Barends, Y. Chen, Z. Chen, B. Chiaro, A. Dunsworth, A. Megrant, P. J. J. O'Malley, C. Neill, P. Roushan, A. Vainsencher, J. Wenner, A. N. Cleland, and John M. Martinis, "Fast accurate state measurement with superconducting qubits," Phys. Rev. Lett. **112**, 190504 (2014).

[10] T. Walter, P. Kurpiers, S. Gasparinetti, P. Magnard, A. Potočnik, Y. Salathé, M. Pechal, M. Mondal, M. Oppliger, C. Eichler, and A. Wallraff, "Rapid high-fidelity single-shot dispersive readout of superconducting qubits," Phys. Rev. Applied **7**, 054020 (2017).

[11] Salvatore S. Elder, Christopher S. Wang, Philip Reinhold, Connor T. Hann, Kevin S. Chou, Brian J. Lester, Serge Rosenblum, Luigi Frunzio, Liang Jiang, and Robert J. Schoelkopf, "High-fidelity measurement of qubits encoded in multilevel superconducting circuits," Phys. Rev. X **10**, 011001 (2020).

[12] D. H. Slichter, R. Vijay, S. J. Weber, S. Boutin, M. Boissonneault, J. M. Gambetta, A. Blais, and I. Siddiqi, "Measurement-induced qubit state mixing in circuit qed from up-converted dephasing noise," Phys. Rev. Lett. **109**, 153601 (2012).

[13] Daniel Sank, Zijun Chen, Mostafa Khezri, J. Kelly, R. Barends, B. Campbell, Y. Chen, B. Chiaro, A. Dunsworth, A. Fowler, E. Jeffrey, E. Lucero, A. Megrant, J. Mutus, M. Neeley, C. Neill, P. J. J. O'Malley, C. Quintana, P. Roushan, A. Vainsencher, T. White, J. Wenner, Alexander N. Korotkov, and John M. Martinis, "Measurement-induced state transitions in a superconducting qubit: Beyond the rotating wave approximation," Phys. Rev. Lett. **117**, 190503 (2016).

[14] Baleegh Abdo, Katrina Sliwa, S Shankar, Michael Hatridge, Luigi Frunzio, Robert J. Schoelkopf, and Michel H. Devoret, "Josephson directional amplifier

for quantum measurement of superconducting circuits," Physical review letters **112**, 167701 (2014).
[15] Leonardo Ranzani and José Aumentado, "Graph-based analysis of nonreciprocity in coupled-mode systems," New Journal of Physics **17**, 023024 (2015).
[16] K. M. Sliwa, M. Hatridge, A. Narla, S. Shankar, L. Frunzio, R. J. Schoelkopf, and M. H. Devoret, "Reconfigurable Josephson circulator/directional amplifier," Phys. Rev. X **5**, 041020 (2015).
[17] F. Lecocq, L. Ranzani, G. A. Peterson, K. Cicak, R. W. Simmonds, J. D. Teufel, and J. Aumentado, "Nonreciprocal microwave signal processing with a field-programmable Josephson amplifier," Phys. Rev. Applied **7**, 024028 (2017).
[18] B. Abdo, N. T. Bronn, O. Jinka, S. Olivadese, A. D. Córcoles, V. P. Adiga, M. Brink, R. E. Lake, X. Wu, D. P. Pappas, and J. M. Chow, "Active protection of a superconducting qubit with an interferometric josephson isolator," Nature communications **5**, 4480 (2019).
[19] F. Lecocq, L. Ranzani, G. A. Peterson, K. Cicak, A. Metelmann, S. Kotler, R. W. Simmonds, J. D. Teufel, and J. Aumentado, "Microwave measurement beyond the quantum limit with a nonreciprocal amplifier," Phys. Rev. Applied **13**, 044005 (2020).
[20] Baleegh Abdo, Oblesh Jinka, Nicholas T. Bronn, Salvatore Olivadese, and Markus Brink, "On-chip single-pump interferometric josephson isolator for quantum measurements," arXiv preprint arXiv:2006.01918 (2020).
[21] F. Lecocq, L. Ranzani, G. A. Peterson, K. Cicak, X. Y. Jin, R. W. Simmonds, J. D. Teufel, and J. Aumentado, "Efficient qubit measurement with a nonreciprocal microwave amplifier," Phys. Rev. Lett. **126**, 020502 (2021).
[22] Joseph Kerckhoff, Kevin Lalumière, Benjamin J. Chapman, Alexandre Blais, and K. W. Lehnert, "On-chip superconducting microwave circulator from synthetic rotation," Phys. Rev. Applied **4**, 034002 (2015).
[23] Eric I. Rosenthal, Benjamin J. Chapman, Andrew P. Higginbotham, Joseph Kerckhoff, and K. W. Lehnert, "Breaking Lorentz reciprocity with frequency conversion and delay," Phys. Rev. Lett. **119**, 147703 (2017).
[24] Benjamin J. Chapman, Eric I. Rosenthal, Joseph Kerckhoff, Bradley A. Moores, Leila R. Vale, J. A. B. Mates, Gene C. Hilton, Kevin Lalumière, Alexandre Blais, and K. W. Lehnert, "Widely tunable on-chip microwave circulator for superconducting quantum circuits," Phys. Rev. X **7**, 041043 (2017).
[25] Benjamin J. Chapman, Eric I. Rosenthal, and K. W. Lehnert, "Design of an on-chip superconducting microwave circulator with octave bandwidth," Phys. Rev. Applied **11**, 044048 (2019).
[26] A. Opremcak, I. V. Pechenezhskiy, C. Howington, B. G. Christensen, M. A. Beck, E. Leonard Jr., J. Suttle, C. Wilen, K. N. Nesterov, G. J. Ribeill, T. Thorbeck, F. Schlenker, M. G. Vavilov, B. L. T. Plourde, and R. McDermott, "Measurement of a superconducting qubit with a microwave photon counter," Science **361**, 1239–1242 (2018).
[27] A. Eddins, J. M. Kreikebaum, D. M. Toyli, E. M. Levenson-Falk, A. Dove, W. P. Livingston, B. A. Levitan, L. C. G. Govia, A. A. Clerk, and I. Siddiqi, "High-efficiency measurement of an artificial atom embedded in a parametric amplifier," Phys. Rev. X **9**, 011004 (2019).
[28] A. Opremcak, C. H. Liu, C. Wilen, K. Okubo, B. G. Christensen, D. Sank, T. C. White, A. Vainsencher, M. Giustina, A. Megrant, B. Burkett, B. L. T. Plourde, and R. McDermott, "High-fidelity measurement of a superconducting qubit using an on-chip microwave photon counter," arXiv preprint arXiv:2008.02346 (2020).
[29] Benjamin J. Chapman, Bradley A. Moores, Eric I. Rosenthal, Joseph Kerckhoff, and K. W. Lehnert, "General purpose multiplexing device for cryogenic microwave systems," Applied Physics Letters **108**, 222602 (2016).
[30] Benjamin J. Chapman, Eric I. Rosenthal, Joseph Kerckhoff, Leila R. Vale, Gene C. Hilton, and K. W. Lehnert, "Single-sideband modulator for frequency domain multiplexing of superconducting qubit readout," Applied Physics Letters **110**, 162601 (2017).
[31] M. Malnou, D. A. Palken, B. M. Brubaker, Leila R. Vale, Gene C. Hilton, and K. W. Lehnert, "Squeezed vacuum used to accelerate the search for a weak classical signal," Phys. Rev. X **9**, 021023 (2019).
[32] Jay Gambetta, W. A. Braff, A. Wallraff, S. M. Girvin, and R. J. Schoelkopf, "Protocols for optimal readout of qubits using a continuous quantum nondemolition measurement," Phys. Rev. A **76**, 012325 (2007).
[33] Ofer Naaman, M. O. Abutaleb, Chris Kirby, and Michael Rennie, "On-chip Josephson junction microwave switch," Applied Physics Letters **108**, 112601 (2016).
[34] Nathan Marchand, "Transmission-line conversion transformers," Electronics **17**, 142–145 (1944).
[35] J. A. B. Mates, G. C. Hilton, K. D. Irwin, L. R. Vale, and K. W. Lehnert, "Demonstration of a multiplexer of dissipationless superconducting quantum interference devices," Applied Physics Letters **92**, 023514 (2008).
[36] M. D. Reed, L. DiCarlo, B. R. Johnson, L. Sun, D. I. Schuster, L. Frunzio, and R. J. Schoelkopf, "High-fidelity readout in circuit quantum electrodynamics using the jaynes-cummings nonlinearity," Phys. Rev. Lett. **105**, 173601 (2010).
[37] M. Malnou, D. A. Palken, Leila R. Vale, Gene C. Hilton, and K. W. Lehnert, "Optimal operation of a josephson parametric amplifier for vacuum squeezing," Phys. Rev. Applied **9**, 044023 (2018).
[38] Waltraut Wustmann and Vitaly Shumeiko, "Parametric resonance in tunable superconducting cavities," Phys. Rev. B **87**, 184501 (2013).
[39] P. Krantz, Y. Reshitnyk, W. Wustmann, J. Bylander, S. Gustavsson, W. D. Oliver, T. Duty, V. Shumeiko, and P. Delsing, "Investigation of nonlinear effects in josephson parametric oscillators used in circuit quantum electrodynamics," New J. Phys. **15**, 105002 (2013).
[40] Waltraut Wustmann and Vitaly Shumeiko, "Parametric effects in circuit quantum electrodynamics," Low Temperature Physics **45**, 848 (2019).
[41] Theodore Van Duzer and Charles William Turner, *Principles of superconductive devices and circuits*, 2nd ed. (Prentice Hall, 1981).
[42] I. Siddiqi, R. Vijay, F. Pierre, C. M. Wilson, M. Metcalfe, C. Rigetti, L. Frunzio, and M. H. Devoret, "Rf-driven josephson bifurcation amplifier for quantum measurement," Phys. Rev. Lett. **93**, 207002 (2004).
[43] V. E. Manucharyan, E. Boaknin, M. Metcalfe, R. Vijay, I. Siddiqi, and M. Devoret, "Microwave bifurcation of a Josephson junction: Embedding-circuit requirements," Phys. Rev. B **76**, 014524 (2007).
[44] Z. R. Lin, K. Inomata, K. Koshino, W. D. Oliver, Y. Nakamura, J. S. Tsai, and T. Yamamoto, "Josephson parametric phase-locked oscillator and its application

to dispersive readout of superconducting qubits," Nature communications **5**, 4480 (2014).

[45] P. Krantz, A. Bengtsson, M. Simoen, S. Gustavsson, V. Shumeiko, W. D. Oliver, C. M. Wilson, P. Delsing, and B. Bylander, "Single-shot read-out of a superconducting qubit using a josephson parametric oscillator," Nature communications **7**, 11417 (2016).

[46] Christian Kraglund Andersen, Joseph Kerckhoff, Konrad W. Lehnert, Benjamin J. Chapman, and Klaus Mølmer, "Closing a quantum feedback loop inside a cryostat: Autonomous state preparation and long-time memory of a superconducting qubit," Phys. Rev. A **93**, 012346 (2016).

[47] A. A. Clerk, M. H. Devoret, S. M. Girvin, Florian Marquardt, and R. J. Schoelkopf, "Introduction to quantum noise, measurement, and amplification," Reviews of Modern Physics **82**, 1155 (2010).

[48] K. Kraus, "General state changes in quantum theory," Ann. Phys. **64**, 311–335 (1971).

[49] C.W. Helstrom, *Quantum detection and estimation theory* (Academic Press: New York, 1976).

[50] Carlton M. Caves, "Quantum limits on noise in linear amplifiers," Phys. Rev. D **26**, 1817–1839 (1982).

[51] D. F. Walls and G. J. Milburn, *Quantum Optics* (Springer, Berlin, 1994).

[52] A. A. Clerk, S. M. Girvin, and A. D. Stone, "Quantum-limited measurement and information in mesoscopic detectors," Phys. Rev. B **67**, 165324 (2003).

[53] Alexander N. Korotkov, "Quantum bayesian approach to circuit qed measurement with moderate bandwidth," Phys. Rev. A **94**, 042326 (2016).

[54] Rui Han, Gerd Leuchs, and Markus Grassl, "Residual and destroyed accessible information after measurements," Phys. Rev. Lett. **120**, 160501 (2018).

[55] C. C. Bultink, B. Tarasinski, N. Haandbæk, S. Poletto, N. Haider, D. J. Michalak, A. Bruno, and L. DiCarlo, "General method for extracting the quantum efficiency of dispersive qubit readout in circuit qed," Applied Physics Letters **112**, 092601 (2018).

[56] For $\sqrt{n_r} \gtrsim 0.2$ our models for both $|\hat{\rho}'_{01}|$ and $F_r$ generally fall within the 95% confidence interval of the measurement, and so only these points are used to obtain efficiency. This choice conservatively affects the reported efficiency: including the first four points, or instead fitting the 'pump on' data, returns a larger value for $\eta$. We note that in this experiment, $\eta$ must be limited to 78% or less based on an independent measurement of loss in the parametric cavity and a model for how this loss affects the efficiency (see supplementary material Section VI.A).

[57] V. B. Braginsky and F. Ya. Khalili, "Quantum nondemolition measurements: the route from toys to tools," Rev. Mod. Phys. **68**, 1–11 (1996).

[58] A. Lupaşcu, S. Saito, T. Picot, P. C. De Groot, C. J. P. M. Harmans, and J. E. Mooij, "Quantum nondemolition measurement of a superconducting two-level system," Nature Physics **3**, 119–123 (2007).

[59] Jay Gambetta, Alexandre Blais, M. Boissonneault, A. A. Houck, D. I. Schuster, and S. M. Girvin, "Quantum trajectory approach to circuit qed: Quantum jumps and the zeno effect," Phys. Rev. A **77**, 012112 (2008).

[60] Aaron D. O'Connell, M. Ansmann, R. C. Bialczak, M. Hofheinz, N. Katz, Erik Lucero, C. McKenney, M. Neeley, H. Wang, E. M. Weig, A. N. Cleland, and J. M. Martinis, "Microwave dielectric loss at single photon energies and millikelvin temperatures," Applied Physics Letters **92**, 112903 (2008).

[61] M. D. Reed, B. R. Johnson, A. A. Houck, L. DiCarlo, Chow J. M., D. I. Schuster, L. Frunzio, and R. J. Schoelkopf, "Fast reset and suppressing spontaneous emission of a superconducting qubit," Applied Physics Letters **96**, 203110 (2010).

[62] Hanhee Paik, D. I. Schuster, Lev S. Bishop, G. Kirchmair, G. Catelani, A. P. Sears, B. R. Johnson, M. J. Reagor, L. Frunzio, L. I. Glazman, S. M. Girvin, M. H. Devoret, and R. J. Schoelkopf, "Observation of high coherence in josephson junction qubits measured in a three-dimensional circuit qed architecture," Phys. Rev. Lett. **107**, 240501 (2011).

[63] Austin G. Fowler, Matteo Mariantoni, John M. Martinis, and Andrew N. Cleland, "Surface codes: Towards practical large-scale quantum computation," Phys. Rev. A **86**, 032324 (2012).

[64] Matthew Reagor, Hanhee Paik, Gianluigi Catelani, Luyan Sun, Christopher Axline, Eric Holland, Ioan M. Pop, Nicholas A. Masluk, Teresa Brecht, Luigi Frunzio, Michel H. Devoret, Leonid Glazman, and Robert J. Schoelkopf, "Reaching 10 ms single photon lifetimes for superconducting aluminum cavities," Applied Physics Letters **102**, 192604 (2013).

[65] Fei Yan, Simon Gustavsson, Archana Kamal, Jeffrey Birenbaum, Adam P. Sears, David Hover, Ted J. Gudmundsen, Danna Rosenberg, Gabriel Samach, S. Weber, Jonilyn L. Yoder, Terry P. Orlando, John Clarke, Andrew J. Kerman, and William D. Oliver, "The flux qubit revisited to enhance coherence and reproducibility," Nature communications **7**, 12964 (2016).

[66] Philipp Kurpiers, Theodore Walter, Paul Magnard, Yves Salathe, and Andreas Wallraff, "Characterizing the attenuation of coaxial and rectangular microwave-frequency waveguides at cryogenic temperatures," . EPJ Quantum Technology **4**, 8 (2017).

[67] G. Calusine, A. Melville, W. Woods, R. Das, C. Stull, V. Bolkhovsky, D. Braje, D. Hover, D. K. Kim, X. Miloshi, D. Rosenberg, A. Sevi, J. L. Yoder, E. Dauler, and W. D. Oliver, "Analysis and mitigation of interface losses in trenched superconducting coplanar waveguide resonators," Applied Physics Letters **112**, 062601 (2018).

[68] Fei Yan, Dan Campbell, Philip Krantz, Morten Kjaergaard, David Kim, Jonilyn L. Yoder, David Hover, Adam Sears, Andrew J. Kerman, Terry P. Orlando, Simon Gustavsson, and William D. Oliver, "Distinguishing coherent and thermal photon noise in a circuit quantum electrodynamical system," Phys. Rev. Lett. **120**, 260504 (2018).

[69] S. Touzard, A. Kou, N. E. Frattini, V. V. Sivak, S. Puri, A. Grimm, L. Frunzio, S. Shankar, and M. H. Devoret, "Gated conditional displacement readout of superconducting qubits," Phys. Rev. Lett. **122**, 080502 (2019).

[70] M. Hatridge, S. Shankar, M. Mirrahimi, F. Schackert, K. Geerlings, T. Brecht, K. M. Sliwa, B. Abdo, L. Frunzio, S. M. Girvin, R. J. Schoelkopf, and M. H. Devoret, "Quantum back-action of an individual variable-strength measurement," Science **339**, 178–181 (2013).

[71] Johannes Heinsoo, Christian Kraglund Andersen, Ants Remm, Sebastian Krinner, Theodore Walter, Yves Salathé, Simone Gasparinetti, Jean-Claude Besse, Anton Potočnik, Andreas Wallraff, and Christopher Eichler, "Rapid high-fidelity multiplexed readout of supercon-

ducting qubits," Phys. Rev. Applied **10**, 034040 (2018).

[72] A. Eddins, S. Schreppler, D. M. Toyli, L. S. Martin, S. Hacohen-Gourgy, L. C. G. Govia, H. Ribeiro, A. A. Clerk, and I. Siddiqi, "Stroboscopic qubit measurement with squeezed illumination," Phys. Rev. Lett. **120**, 040505 (2018).

[73] T. Thorbeck, S. Zhu, E. Leonard Jr., R. Barends, J. Kelly, John M. Martinis, and R. McDermott, "Reverse isolation and backaction of the slug microwave amplifier," Physical Review Applied **8**, 054007 (2017).

[74] Christian Kraglund Andersen, Ants Remm, Stefania Lazar, Sebastian Krinner, Johannes Heinsoo, Jean-Claude Besse, Mihai Gabureac, Andreas Wallraff, and Christopher Eichler, "Entanglement stabilization using ancilla-based parity detection and real-time feedback in superconducting circuits," npj Quantum Information **5**, 69 (2019).

[75] Christian Kraglund Andersen, Ants Remm, Stefania Lazar, Sebastian Krinner, Nathan Lacroix, Graham J. Norris, Mihai Gabureac, Christopher Eichler, and Andreas Wallraff, "Repeated quantum error detection in a surface code," Nature Physics **16**, 875880 (2020).

[76] T. Peronnin, D. Marković, Q. Ficheux, and B. Huard, "Sequential dispersive measurement of a superconducting qubit," Phys. Rev. Lett. **124**, 180502 (2020).

[77] D. Rosenberg, D. Kim, R. Das, D. Yost, S. Gustavsson, D. Hover, P. Krantz, A. Melville, L. Racz, G. O. Samach, S. J. Weber, F. Yan, J. L. Yoder, A. J. Kerman, and W. D. Oliver, "3d integrated superconducting qubits," npj Quantum Inf **3**, 42 (2017).